

TABLE I. Fractional change in length vs temperature.

$T^{\circ}\text{C}$	$\Delta l/l_{25} \times 10^4$	$T^{\circ}\text{C}$	$\Delta l/l_{25} \times 10^4$
25.0	0	213.6	11.62
33.3	0.43	239.3	13.31
46.9	1.21	264.3	14.93
59.8	1.95	288.6	16.59
72.2	2.69	313.8	18.30
69.5	2.56	338.2	19.93
81.8	3.29	213.5	11.59
94.2	4.03	251.9	14.15
111.4	5.08	276.6	15.84
136.8	6.64	300.87	17.50
162.3	8.27	326.25	19.24
187.9	9.94	175.23	9.05

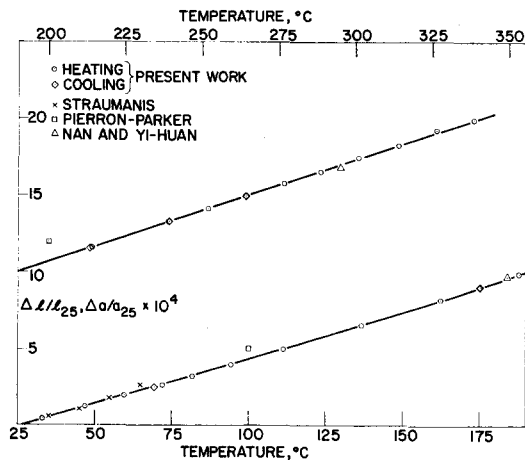


FIG. 1. Length and lattice parameter expansion of GaAs vs temperature. Lower and upper curves are associated with the lower and upper temperature scales respectively. Diamonds and circles represent present work. Crosses, squares, and triangles represent lattice-parameter measurements reported by others.

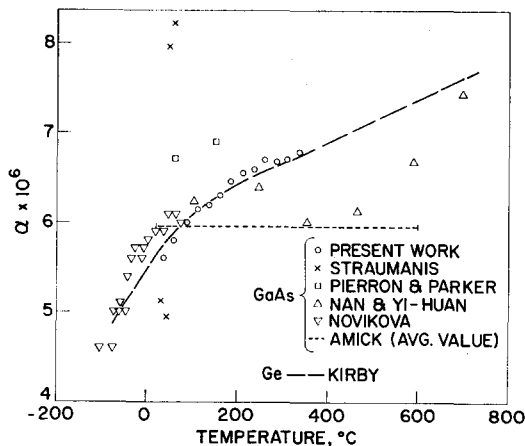


FIG. 2. Coefficient of thermal expansion of single-crystal GaAs and polycrystalline Ge vs temperature. Solid circles represent present work. Apart from Novikova's data (inverted triangles) on the thermal expansion of GaAs, the remaining data are from x-ray measurements. The dashed line represents the thermal expansion coefficient of polycrystalline Ge according to Kirby.

lower and upper scales, respectively. Wherever possible, the experimental values reported by other investigators are also plotted on the same graph. (x-ray results are plotted in terms of the fractional change in the lattice parameter, a .) Where necessary, the data of other workers have been adjusted by interpolation to the common reference temperature of 25°C .

Since some previous workers have expressed their results only in terms of the expansion coefficient α , all results are shown in this form in Fig. 2. The present experimental data was reduced to this form using intervals of 25°C to compute α ; the estimated accuracy for these values of α is $\pm 0.5 \times 10^{-7}$.

It can be seen that the only reasonable agreement among the GaAs data is that between Novikova and the present results. For comparison purposes, the thermal expansion of polycrystalline Ga as given by Kirby⁷ has been shown in Fig. 2 by the broken line. The addition of the present results to those of Novikova make it apparent that the expansion behavior of single-crystal semi-insulating GaAs is a good match to that reported for polycrystalline Ge over a considerable range of temperatures.

¹ M. E. Straumanis and C. D. Kim, *Acta Cryst.* **19**, 256 (1965).

² E. D. Pierron, D. L. Parker, and J. B. McNeely, *Acta Cryst.* **21**, 290 (1966).

³ J. A. Amick, *RCA Rev.* **24**, 555 (1963).

⁴ S. Nan and L. Yi-huan, *Scientia Sinica* **14**, 1582 (1965).

⁵ S. I. Novikova, *Sov. Phys.—Solid State* **3**, 129 (1961).

⁶ R. Feder and H. Charbneau, *Phys. Rev.* **149**, 464 (1966).

⁷ R. K. Kirby, *AIP Handbook*, 2nd ed. (1963), pp. 4-64.

The Three-Dimensional Poole-Frenkel Effect

J. L. HARTKE*

Xerox Corporation, Webster, New York

(Received 27 November 1967; in final form 3 May 1968)

Electric-field-assisted thermal ionization of trapped charge carriers in electronic semiconductors and insulators was initially described by Frenkel,¹ who estimated the effect of the field on electrical conductivity to be

$$\sigma = \sigma_0 \exp(\beta \sqrt{\epsilon/kT}), \quad (1)$$

$$\beta = (e^2/\pi K \epsilon_0)^{1/2}. \quad (2)$$

The parameter σ_0 is the low-field conductivity; ϵ is the applied electric field; e and ϵ_0 are the electronic charge and permittivity of free space, respectively, in rationalized *mks* units [$\epsilon_0 = (36\pi \times 10^9)^{-1}$ F/m], and K is the relative high-frequency dielectric constant. The results of current-voltage measurements^{2,3} on thick films of SiO_2 , Al_2O_3 , and Ta_2O_5 are in qualitative agreement with the field and temperature dependences predicted by Eq. (1). However, the resulting constant β has been somewhat smaller than values obtained using Eq. (2) and has occasionally been in near agreement with the Schottky effect which assumes field-assisted thermal excitation of charge carriers across a planar metal-insulator contact

$$\sigma = \sigma_0 \exp(\frac{1}{2}\beta \sqrt{\epsilon/kT}). \quad (3)$$

The factor $\frac{1}{2}$ in the exponent arises from the interaction of the charge carrier with its image charge rather than with the spatially fixed charge assumed by Frenkel in obtaining Eq. (1).

Since experimental results seem to fall between the predictions of Eqs. (1) and (3), theorists have attempted to explain the results by introducing multiple trapping effects. Both Fowler-Nordheim (cold-cathode tunneling) and Schottky emission have been treated by O'Dwyer,⁴ while Simmons⁵ has modified Frenkel's original model. It has not been widely recognized that Frenkel's estimate was based on a one-dimensional (planar) model, and it will now be shown that a three-dimensional treatment predicts field and temperature dependences which are different from Eqs.

(1) and (2). Although the assumptions required to obtain a simple result prevent an exact treatment of the Poole-Frenkel effect, the results obtained do provide an improved basis for comparison with experiment.

The electrostatic energy of an electron which is attracted to a singly charged positive ion located at $r=0$ and is under the influence of a uniform applied field \mathcal{E} in the $-z$ direction may be written as

$$E = -(e^2/4\pi K\epsilon_0 r) - e\mathcal{E}r \cos\theta, \quad (4)$$

where rationalized mks units and spherical coordinates are used and the arbitrary zero of energy is taken to be the bottom of the conduction band at $r=0$. As shown by Fig. 1, the thermal energy which a trapped electron must gain in order to escape is reduced by an amount δE which is obtained by setting $\partial E/\partial r=0$ at $r=r_0$.

The result is

$$r_0 = (e^2/4\pi K\epsilon_0 \mathcal{E} \cos\theta)^{1/2}, \quad (5)$$

$$\delta E = (e^3 \mathcal{E} \cos\theta / \pi K\epsilon_0)^{1/2}, \quad (6)$$

where the barrier is lowered only for $0 \leq \theta \leq \pi/2$. The release rate, or reciprocal lifetime, of a trapped electron may be obtained by assuming a spherically symmetric, field independent, attempt-to-escape frequency of $\nu/4\pi$ per unit solid angle and by assuming that the release rate is field independent⁶ for $\pi/2 \leq \theta \leq \pi$.

$$(\tau_r)^{-1} = \int_0^{2\pi} d\phi \int_0^{\pi/2} d\theta \sin\theta (\nu/4\pi) \exp[-(E_T - \delta E)/kT] \\ + \int_0^{2\pi} d\phi \int_{\pi/2}^{\pi} d\theta \sin\theta (\nu/4\pi) \exp(-E_T/kT). \quad (7)$$

The integrals may be evaluated by substituting $t = \cos\theta$, the result being

$$\tau_{r0}/\tau_r = (kT/\beta\sqrt{\mathcal{E}})^2 \{1 + [(\beta\sqrt{\mathcal{E}}/kT) - 1] \exp(\beta\sqrt{\mathcal{E}}/kT)\} + \frac{1}{2}, \quad (8)$$

where the zero-field release rate, $(\tau_{r0})^{-1}$, is $\nu \exp(-E_T/kT)$ and β is defined by Eq. (2).

The field-enhanced conductivity⁷ may be obtained by assuming that the mobility and the capture rate, or free lifetime, of conduction electrons is field independent, and by assuming that the density of occupied electron traps is reduced a negligible amount by the field.

$$\sigma = \sigma_0 (\tau_{r0}/\tau_r). \quad (9)$$

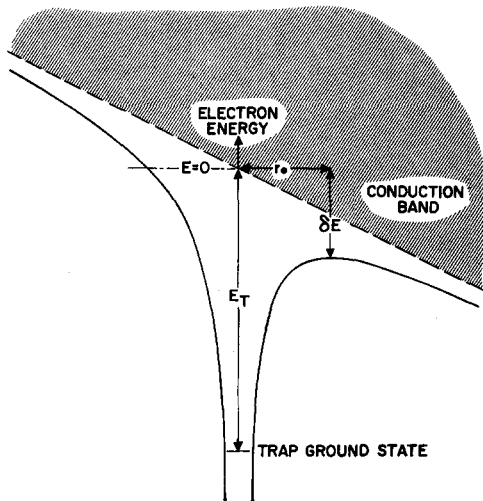


FIG. 1. Energy of an electron bound to a positive point charge in the presence of a uniform applied field.

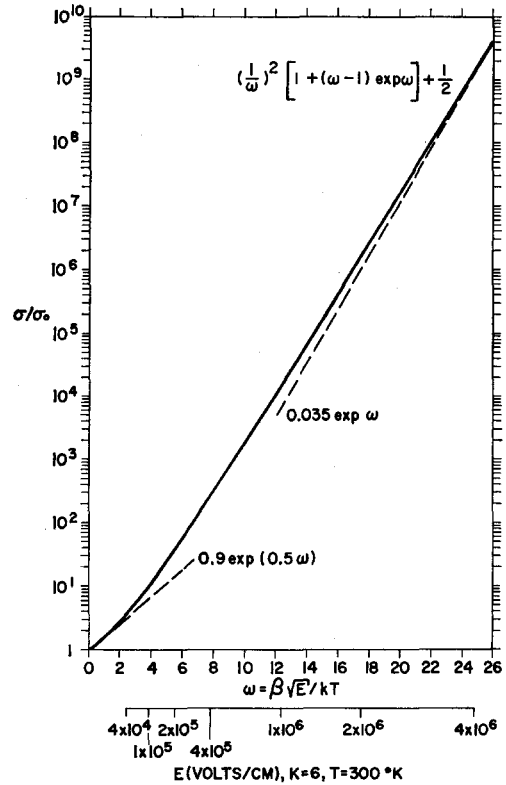


FIG. 2. Enhanced electrical conductivity expected for field-assisted thermal ionization of electrons trapped by a positive point charge.

Thus the field- and temperature-dependent conductivity is described by Eq. (8) which approaches

$$\sigma/\sigma_0 \approx (kT/\beta\sqrt{\mathcal{E}}) [1 - (kT/\beta\sqrt{\mathcal{E}})] \exp(\beta\sqrt{\mathcal{E}}/kT) \quad (10)$$

at high fields and should be readily distinguishable from the dependences predicted by Eqs. (1) or (3), particularly since values of $\beta\sqrt{\mathcal{E}}/kT$ in excess of ten are attainable.^{2,3} The conductivity predicted by Eqs. (8) and (9) is shown in Fig. 2, from which it is apparent that the force-fitting of this curve to an exponential would produce a result which depended strongly upon the maximum field attained and which varied between the predictions of Eqs. (1) and (3). In contrast to the slowly varying potential of the Coulomb center, a spherically symmetric square well potential of radius b leads to a more rapid increase of conductivity with increasing electric field.

$$\sigma/\sigma_0 = (kT/2e\mathcal{E}b) [\exp(e\mathcal{E}b/kT) - 1] + \frac{1}{2}. \quad (11)$$

The assumptions inherent to the above calculations may not be fully justified at high fields, particularly in regards to the field independent mobility. If the conduction electron drift velocity reaches a field independent saturation value, then Eq. (9) should be multiplied by a factor proportional to $(\mathcal{E})^{-1}$ at high fields. This would cause the conductivity shown in Fig. 2 to approach more closely a simple exponential behavior. The mean free time before capture of the conduction electrons could also change at high fields, particularly if capture was initially into shallow bound states. It can be seen from Fig. 1 that very shallow levels are nonlocalized at high fields, leading to a possible increase in the free lifetime of electrons.

* Present address: Ion Physics Corporation, Burlington, Mass. 01803.

¹ J. Frenkel, Tech. Phys. USSR 5, 685 (1938); Phys. Rev. 54, 647 (1938).

² T. E. Hartman *et al.*, J. Appl. Phys. **37**, 2468 (1966), and references cited therein.

³ I. T. Johansen, J. Appl. Phys. **37**, 499 (1966).

⁴ J. J. O'Dwyer, J. Appl. Phys. **37**, 599 (1966).

⁵ J. G. Simmons, Phys. Rev. **155**, 657 (1967).

⁶ This assumption is unimportant in the low-field and high-field limits.

⁷ A similar result is obtained for macroscopic drift mobilities which are limited by multiple trapping.

$S=1.48$, which, considering the approximations involved, is reasonably close to $\frac{2}{3}$.

¹ V. P. Koryavov, J. Appl. Mech. Theoret. Phys. (PMTF) No. 5, 123 (1964).

² V. M. Gogolev, V. G. Mirkin, and G. I. Yablokova, J. Appl. Mech. Theoret. Phys. (PMTF), No. 5, 93 (1963).

³ J. J. Gilvarry, Phys. Rev. **102**, 325 (1956).

⁴ J. Berger and S. Joigneau, Compt. Rend. **249**, 2506 (1959).

⁵ A. L. Ruoff, J. Appl. Phys. **38**, 4976 (1967).

Correlation of Two "Universal" Hugoniot

JAMES F. HEYDA

General Electric Co., King of Prussia, Pennsylvania

(Received 5 April 1968; in final form 9 May 1968)

Koryavov¹ and Gogolev, Mirkin, and Yablokova² have proposed distinct representations of "universal" Hugoniot for the shock compression of metals, rocks, and other nonporous solids based on correlating a large quantity of experimental data for these materials.

The results from Refs. 1 and 2 are given by Eqs. (1) and (2), respectively,

$$D = c_0 + \frac{2}{3}u, \quad (1)$$

$$p = (\rho_0 c_0^2 / 5.5) [(\rho/\rho_0)^5 - 1], \quad (2)$$

where D is the speed of a planar shock wave in the material and u , p , and ρ are, respectively, the particle speed, pressure, and density directly back of the shock; ρ_0 is the normal density of the material and c_0 is an experimental constant, close to the sonic velocity in the material.

It is the purpose of this note to point out that the constants $\frac{2}{3}$ and 5 are but a special instance of the pair S and $4S-1$, which follows naturally from a result of Gilvarry.³

We note first that the Grüneisen coefficient at normal density, Γ_0 , implied by the Landau-Slater relation for the Grüneisen coefficient $\Gamma(\rho)$ and the particular choice of Hugoniot, $D = c_0 + Su$ is given by⁴

$$\Gamma_0 = 2(S - \frac{1}{3}). \quad (3)$$

However, Gilvarry³ has shown that for the Murnaghan form of the Hugoniot,

$$p = A[(\rho/\rho_0)^n - 1], \quad (4)$$

the exponent n is given by

$$n = 2\Gamma_0 + \frac{1}{3}. \quad (5)$$

From (3) and (5) then we find $n = 4S - 1$. Thus, the Murnaghan Hugoniot "compatible" with the Hugoniot $D = c_0 + Su$ is

$$p = [A(\rho/\rho_0)^{4S-1} - 1]. \quad (6)$$

An independent derivation of this fact appears in a paper by Ruoff⁵ who proceeds *ab initio* by equating the pressure in (4), with ρ/ρ_0 replaced by its Hugoniot equivalent $D/(D-u)$ from the conservation of mass relation, to $\rho_0 Du$ (conservation of momentum relation) and then, in the resulting equation, expresses D as a Maclaurin series in u . Expanding both members of the equation in series and comparing coefficients of equal powers of u , one then obtains $n = 4S - 1$ directly.

An additional check on this $S \leftrightarrow 4S - 1$ correspondence is furnished by the formula, derived in Ref. 2, for the Brüneisen coefficient $\Gamma(\rho)$:

$$\Gamma(\rho) = 2.3(\rho/\rho_0)^{-1.23}. \quad (7)$$

From (7) we find $\Gamma(\rho_0) = \Gamma_0 = 2.3$, which implies, using (3), that

Electron-Drift Mobility in Single-Crystal HgS

MARK D. TABAK AND GARETH G. ROBERTS

Research Laboratories, Xerox Corporation, Rochester, New York 14580

(Received 27 May 1968)

The mobilities of most II-VI semiconductors possessing either the zinc blende or wurtzite structure are well documented.¹ However, very little information is available for mercury sulfide, whose stable form at room temperature has D_{3d} symmetry, which makes it the diatomic analog of the trigonal elemental semiconductors, Se and Te. In this note, we describe two independent determinations of the electron-drift mobility of natural single-crystal HgS (Mexican cinnabar) whose resistivity $\sim 10^{12} \Omega \cdot \text{cm}$. The crystals were of high chemical purity; semiquantitative spectrographic analysis showed less than 25 ppm Fe and Si, and less than 5 ppm Al, Cu, and Mg. X-ray diffraction studies and optical measurements indicated excellent crystalline quality.

Because of the problems associated with electrical measurements in highly insulating photoconductors, a conventional Hall-effect experiment was not feasible for this compound. Accordingly, we adopted two other techniques, both of which were well suited

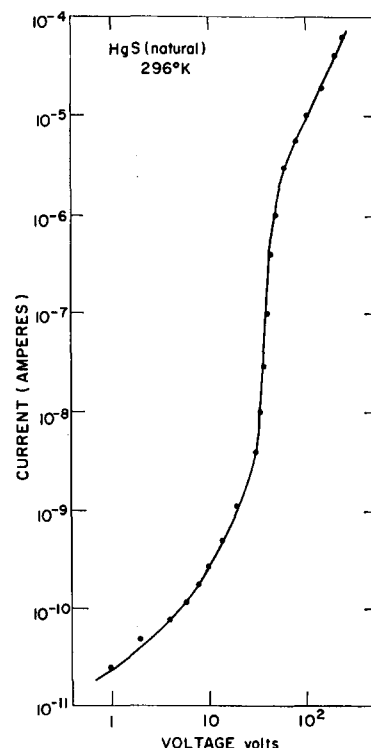


FIG. 1. Current-voltage curve for natural single-crystal HgS: $L = 0.3 \text{ mm}$; electrode area = 2 mm^2 .